

# **Adaptive flexibility of cytoskeletal structures through nonequilibrium entropy production**

**Yuika Ueda<sup>1</sup> and Shinji Deguchi<sup>1,\*</sup>**

<sup>1</sup> Division of Bioengineering, Graduate School of Engineering Science, Osaka University

\* Corresponding author

Address: 1-3 Machikaneyama, Toyonaka, Osaka 560-8531, Japan

E-mail: [deguchi.shinji.es@osaka-u.ac.jp](mailto:deguchi.shinji.es@osaka-u.ac.jp)

Phone: +81 6 6850 6215

ORCID: 0000-0002-0556-4599

## **Abstract**

Cellular adaptation to environmental changes relies on the dynamic remodeling of cytoskeletal structures. Sarcomeres, periodic units composed mainly of actin and myosin II filaments, are fundamental to the function of the cytoskeletal architecture. In muscle cells, sarcomeres maintain consistent lengths optimized for stable force generation, while in nonmuscle cells, they display greater structural variability and undergo adaptive remodeling in response to environmental cues. However, the relevance of this structural variability to cellular adaptability remains unclear. Here, we present a nonequilibrium physics framework to investigate the role of sarcomere variability in cytoskeletal adaptation. By deriving the probability distribution of sarcomere lengths and analyzing binding energies during cytoskeletal elongation, we show that structural variability, rather than hindering function, facilitates adaptive responses to environmental conditions. We reveal that entropy production arising from this variability drives dynamic remodeling, allowing the cytoskeletal architecture to respond effectively to external cues. This framework bridges sarcomere variability and cytoskeletal adaptability required for diverse cellular functions, providing new insights into how variability supports cellular adaptation through nonequilibrium processes.

# 1. Introduction

Living cells adapt their internal structures in response to changes in both their internal and external environments (1,2). This adaptability is fundamental to individual cellular processes such as differentiation, proliferation, and apoptosis, as well as to higher-order processes such as tissue development and wound healing (3,4). The cytoskeleton is central to the physical structure and force generation of cells, maintaining its integrity through organized protein complexes. Among these, the sarcomere, a periodic structure primarily composed of actin and myosin II filaments, functions as the fundamental unit of the cellular cytoskeletal architecture.

While sarcomeres are well defined in muscle cells (5–9), similar structures are also found in nonmuscle cells (10–18). Compared to the consistent sarcomere length and alignment in muscle cells, nonmuscle sarcomeres exhibit greater structural variability; and even within muscle cells, younger ones display more randomness than mature ones (19). This variability is more pronounced in motile cells than in nonmotile cells, which possess different potentials for movement and proliferation (11,12). Muscle sarcomeres are optimized for force generation within muscle tissues (5), while nonmuscle sarcomeres are involved in diverse dynamic cellular processes such as division, migration, and structural remodeling upon environmental changes (20–23).

Traditionally, these differences in sarcomere structures have been attributed to the unique properties of proteins expressed in each cell type, often within a reductionist framework. On the other hand, to achieve a unified understanding of how this architectural randomness is inherently linked to distinct cellular functions, a comparative approach based on physical principles is essential. In this regard, prior studies from a physical perspective have aimed to elucidate the mechanisms for the self-organization of sarcomere periodicity (20,21,24,25), with some attempts in exploring how ATP-driven actomyosin contractions generate cellular tension and in turn maintain sarcomere structures (5,26,27). However, the potential link between sarcomere variability and cellular functions including adaptability remains unclear.

Here, we develop a theoretical framework to describe the relationship between sarcomere structural variability and cellular adaptability from a nonequilibrium physics perspective. Specifically, we derive constraints on the probability distribution of sarcomere structures and the binding energy among sarcomeres, illustrating how variability may enhance adaptability. Given that ATP-dependent processes represent nonequilibrium phenomena, we incorporate relevant biophysical properties into a Fokker–Planck equation to derive the probability distribution of sarcomere configurations. We then

quantify entropy production to evaluate the energetic cost of maintaining these structures. Our results clarify a fundamental physical principle, demonstrating that the structural properties of sarcomeres, often considered at the level of individual contractile units, enhance cellular adaptability at larger scales. Interestingly, the inherent randomness in sarcomere structure, which impairs function in engineered systems, may instead promote the unique adaptability of living organisms.

## 2. Model

### 2.1 Probability distribution of sarcomere structures

The sarcomere is the intracellular contractile unit with a certain periodic structure, along which actin, myosin, and  $\alpha$ -actinin appear in a cell type-dependent probability distribution (Fig. 1). Nonmuscle cells tend to express sarcomeres that are more spatially irregular compared to those in muscle cells. We model the sarcomere in a one-dimensional framework, defining the probability of its length state  $x$  as  $P(x)$ . Given the biophysical property of the sarcomere response, which is convex downward with respect to the stable length  $x_0$ , the potential energy  $U(x)$  at sarcomere length  $x$  is given by

$$U(x) = \frac{1}{2}k(x - x_0)^2 \quad (1)$$

where  $k$  represents the restoring contribution of the sarcomere. Using the Fokker-Planck equation, the time evolution of  $P(x, t)$  is described by

$$\frac{\partial P(x, t)}{\partial t} = -\frac{\partial}{\partial x} \{-k(x - x_0)P(x, t)\} + \frac{\partial^2}{\partial x^2} \{DP(x, t)\} \quad (2)$$

where  $D$  is the diffusion coefficient. By solving Eq. (2) under the steady-state condition, we obtain the stationary probability distribution as

$$P(x) = \frac{\exp\left(-\frac{k(x-x_0)^2}{2D}\right)}{\sum \exp\left(-\frac{k(x-x_0)^2}{2D}\right)} \quad (3)$$

where  $P(x)$  satisfies the normalization condition  $\sum P(x) = 1$ .

## 2.2 Entropy production

We consider the cytoskeletal structure with sarcomeres as the system and the surrounding environment as the heat bath. We quantify the nonequilibrium entropy production during the growth process of the cytoskeletal structure while nearby sarcomeres bind together or unbind. In actual cells, the cytoskeletal growth occurs at the level of individual proteins, namely actin, myosin, and  $\alpha$ -actinin, rather than at the whole sarcomere level, but we simplify this process by modeling the combined action of these proteins as equivalent to sarcomere level binding. We assume that the environment is large enough to remain close to thermal equilibrium. The total entropy production, considered for both the system and the environment, is defined as

$$\sigma = \Delta S_{sys} + \Delta S_{bath} \geq 0 \quad (4)$$

where  $\Delta S_{sys}$  and  $\Delta S_{bath}$  are the change in entropy of the system and of the surrounding environment, respectively (28).

In nonequilibrium systems,  $\Delta S_{sys}$  can be expressed using Shannon entropy as follows (26):

$$\Delta S_{sys} = - \sum P(x) \ln P(x). \quad (5)$$

For  $\Delta S_{bath}$ , we assume that the environment can freely exchange sarcomere elements and energy with the preexisting cytoskeletal structure and is therefore described by a grand canonical distribution under

this theoretical assumption. The change in entropy of the environment is given by

$$\Delta S_{bath} = -\beta(\Delta E - \Delta\mu) \quad (6)$$

where  $\Delta E$  is the energy change in the cytoskeletal structure due to sarcomere binding,  $\Delta\mu$  is the change in chemical potential as sarcomeres transition from the particle bath to within the cytoskeletal structure, and  $\beta=1/k_bT$  representing the inverse thermal energy. Using Eqs. (5) and (6), the total entropy production is expressed by

$$\sigma = -\sum P(x)\ln P(x) - \beta(\Delta E - \Delta\mu) \geq 0, \quad (7)$$

showing that the entropy production during the forming process of the cytoskeletal structure is always positive.

### 2.3 Maximum binding energy

We define  $\Delta E$  in Eq. (6) as the energy change due to sarcomere binding to the cytoskeletal structure, corresponding to the binding energy, or  $\Delta E = \Delta E^b$ . From Eq. (7), the binding energy is defined as

$$\Delta E^b \leq \Delta E_{max}^b = \Delta\mu - \frac{1}{\beta} \sum P(x)\ln P(x). \quad (8)$$

Based on the second law of thermodynamics, the nonequilibrium forming of the cytoskeletal structure driven by sarcomere binding consistently generates positive entropy. This constraint imposes a limit on the binding energy, determined by the chemical potential and the entropy associated with the underlying randomness of the sarcomere structure. In particular, the binding energy represents the strength of the interaction between sarcomeres, with a more negative binding energy indicating a stronger binding. We quantitatively analyzed the maximum binding energy  $\Delta E_{max}^b$  with the

probability distribution of sarcomere structures (Eq. 3). Each parameter used is determined based on experimental data, with  $D = 10 \mu\text{m}^2/\text{s}$  and  $T = 310.15 \text{ K}$  (29–33), and  $\Delta\mu$  was estimated to be on the order of 20 kJ/mol from experimental measurements of the energy associated with ATP hydrolysis (34,35).

## 2.4 Quantification of sarcomere length

The actual sarcomere length was quantified using previously published experimental images from multiple sources, including mouse skeletal muscles (36), primary mice myotubes (37), neonatal rat cardiomyocytes (38), and myofibrils isolated from rabbit glycerinated psoas muscle fibers in a rigor state (39), which predominantly express striated muscle-type actin and myosin molecules; and human fibroblasts (40), PtK2 long-nosed potoroo epithelial kidney cells (40), gerbil fibroma cells (40), and A7r5 rat aortic smooth muscle cells (41), which express nonstriated muscle-type actin and myosin molecules. Among them, A7r5 cells also express  $\alpha$ -SMA, a smooth muscle-specific actin isoform commonly used as a marker for smooth muscle cells and myofibroblasts. Images of endogenous  $\alpha$ -actinin immunostaining (37,38,40,41), transmission electron microscopy images (37), or phase-contrast microscopy images (39) were analyzed by using ImageJ/Fiji software (NIH). Lines were drawn along the longitudinal axis of multiple sarcomeres, and the intensity profile was examined to measure the distance between peaks, which correspond to sarcomere length. The lengths of  $n = 40\text{--}48$  sarcomeres in striated muscle types and  $n = 53\text{--}56$  sarcomeres in nonstriated muscle types were analyzed to obtain the respective distributions.

## 3. Results

### 3.1 Analysis of sarcomere length variability

The probability distribution for sarcomere lengths was analyzed using our model (Eq. 3) (Fig. 2). These distributions follow a Gaussian distribution with variance  $\sqrt{D/k}$ , influenced by both noise and restoring contribution. As  $k$  increases, representing greater contractile force maintained within the cytoskeletal structure, the variance decreases, resulting in sarcomeres being more stably distributed around a specific length. Conversely, as  $k$  decreases, the variance increases, leading to a broader length distribution and a more random sarcomere structure. This behavior is consistent with experimentally observed properties in muscle and nonmuscle cells. Specifically, in mouse skeletal

muscles (hereafter referred to Skeletal muscles), primary mice myotubes (Myotubes), neonatal rat cardiomyocytes (Cardiomyocytes), and myofibrils isolated from rabbit glycerinated psoas muscle fibers in a rigor state (Skeletal myofibrils), which all predominantly express striated muscle-type actin and myosin molecules and are characterized by high contractile force, sarcomeres are consistently observed to maintain a specific length (Fig. 3); to clearly demonstrate this observation, Shannon entropy was calculated for each distribution. In contrast, in human fibroblasts (Fibroblasts), PtK2 long-nosed potoroo epithelial kidney cells (PtK2 cells), and gerbil fibroma cells (Fibroma cells), which express nonstriated muscle-type actin and myosin molecules and are characterized by less contractile force, sarcomeres exhibit greater length variability. Thus, nonmuscle sarcomeres show a relatively random structure compared to those in muscle cells, while still maintaining a characteristic stable length (15,42). A7r5 rat aortic smooth muscle cells (A7r5 cells), which express both  $\alpha$ -SMA and muscle-type  $\alpha$ -actin, exhibit intermediate randomness between muscle-type and nonmuscle-type.

### 3.2 Analysis of maximum binding energy

Our analysis shows that the maximum binding energy decreases as the restoring contribution increases, indicating that the impact of the binding energy associated with the extent of sarcomere interactions increases under these conditions (Fig. 4a). This occurs because, as the restoring contribution increases, and the sarcomere structure becomes more ordered, the influence of entropy is reduced (Fig. 2, blue), thus allowing the binding energy to exert greater dominance in driving cytoskeletal elongation. On the other hand, when the restoring contribution is small, the resulting more disordered sarcomere configuration (Fig. 2, red) reduces the dominance of the binding energy, allowing sarcomere assembly to occur more easily and enabling more flexible cytoskeletal remodeling. These findings suggest that cytoskeletal structures with random sarcomere arrangements, as observed in nonmuscle cells, are better adaptable for dynamic elongation. In contrast, cytoskeletal structures with ordered sarcomeres, such as those in muscle cells, requires higher change in binding energy for elongation, indicating that such systems are less suited for dynamic elongation while maintaining their structural integrity. Interestingly, the value of  $x_0$  does not affect the limits of the binding energy because entropy is determined not by the absolute sarcomere stable length but by the probability of the structure being randomly distributed.

The relationship with the chemical potential reveals a positive correlation with the maximum binding energy as explicitly described in Eq. 9 (Fig. 4b). A small difference in chemical potential (Fig. 4b, red regions) corresponds to a reduced impact of the binding energy, facilitating easier remodeling



of the structures. While our discussion has focused on the extent of the sarcomere randomness, it should be noted that chemical potential depends on component concentration, which varies with intracellular environmental conditions. Therefore, even with the same randomness in sarcomere structures, the behavior is actually influenced by environmental factors including concentration.

The binding energy for different types of sarcomere structures was estimated using Eq. (8) and actual measurements of the distribution (Fig. 3), showing its proportionality to the change in system entropy at a fixed chemical potential,  $-20$  kJ/mol (Fig. 5). The nonmuscle sarcomeres tend to have lower levels of binding energy compared to muscle sarcomeres, indicating that the former can remodel their structures more easily than the latter.

## 4. Discussion

In this work, we developed a nonequilibrium physical model to elucidate how the biophysical properties of sarcomeres influence cytoskeletal stability (Fig. 4). Previous studies have largely focused on self-organizing mechanisms of sarcomere patterning, but it remained unclear how sarcomere characteristics are associated with cellular adaptability (20,21,24,25). We modeled the probability distribution of sarcomere length by integrating essential physical factors such as restoring mechanisms and fluctuations into an energy model. Using the Fokker-Planck equation, we derived the probability distribution of sarcomere lengths (Eq. (3)), revealing that higher restoring forces produce narrower distributions with less random structural variations around a specific length. This finding is consistent with experimental observations, in which muscle cells with high contractile forces exhibit ordered sarcomere structures, whereas nonmuscle cells with weaker contractile forces display more dispersed configurations (5,10–17,43,44). Interestingly, cytoskeletal stiffness increases with cellular aging, accompanied by reduced sarcomere distributions (45), potentially reflecting a decline in cellular adaptability during maturation.

We applied a nonequilibrium framework to determine the entropy production during cytoskeletal remodeling due to sarcomere binding. Sarcomeres generate contractile forces via ATP-driven actomyosin activity, creating a nonequilibrium system with continuous energy flux. In our model, we considered the cytoskeletal structure composed of sarcomeres as the system and its surrounding environment as the reservoir. Given that sarcomere binding allows for cytoskeletal elongation, we modeled the environment as a grand canonical ensemble and quantified the resulting entropy production. By determining Shannon entropy (46) from the probability distribution of sarcomere

lengths, we derived a limit on binding energy (Eq. (9)), constrained by the requirement of nonnegative entropy production in nonequilibrium systems (28). Our analysis then provided a mechanism, by which the maximum binding energy is influenced by structural randomness. In muscle cells with high restoring force and ordered sarcomere lengths, the requirement for entropy production necessitates substantial binding energy for cytoskeletal elongation. In contrast, in nonmuscle cells with lower restoring force and more random sarcomere lengths, the entropy resulting from sarcomere disorder allows for more flexible cytoskeletal remodeling with minimal binding energy. Thus, these cytoskeletal structures achieve high adaptability, or flexible responsiveness to environmental cues, facilitated by the entropy contributed by sarcomere randomness. Interestingly, young muscle cells display greater randomness in sarcomeres than mature cells (19), potentially suggesting that early-stage cells may be more adaptable and then gradually form specialized structures optimized for stable contractile force generation as they mature. Note that binding energy is also modulated by the chemical potential, which depends on intracellular component concentrations, influencing the resulting structure. For example, in high ATP environments, stable cytoskeletal structures with strong binding energies can form even in presence of random sarcomere structures. Thus, cytoskeletal structures can remodel in response to conditions within the system as well as those in the environment. Our theoretical description captures this cellular behavior, aligning with experimentally observed relationships across the different hierarchies, namely between sarcomeres and cells (5,10–17,43).

While we have primarily discussed the qualitative relevance of sarcomere structures to cellular adaptability, we also estimated the binding energy for different types of sarcomere structures (Fig. 5). We found that the estimated tendency is consistent with experimental observations. Specifically, nonmuscle  $\alpha$ -actinin isoforms have been reported to exhibit higher dissociation constants  $K_d$  for actin binding, ranging from 2.96 to 3.96  $\mu\text{M}$  (47), compared to muscle  $\alpha$ -actinin isoforms, which show lower  $K_d$  values of 0.4  $\mu\text{M}$  (48) or 0.59  $\mu\text{M}$  (49). This difference suggests that muscle  $\alpha$ -actinin binds actin more stably, stabilizing the sarcomere more effectively than nonmuscle  $\alpha$ -actinin. Regarding myosin, another major actin cross-linker, the  $K_d$  value of muscle myosin isoforms (28.2 nM) is higher than that of nonmuscle myosin ones (4.6 nM) (50), suggesting a higher affinity of nonmuscle myosin for actin. Functionally, muscle myosin molecules undergo rapid cross-bridging cycles to facilitate muscle contraction, whereas nonmuscle myosin molecules remain attached to actin to sustain cellular tension along stress fibers. These distinct roles suggest that  $\alpha$ -actinin, rather than myosin, predominantly drives the remodeling activity of sarcomere structures.

In conclusion, we developed a physical framework linking different hierarchical processes, namely sarcomere randomness and cellular adaptability, from a nonequilibrium perspective. We

suggest that structural disorder, often perceived as disadvantageous, actually enhances cellular adaptability by increasing entropy. This randomness is not limited to sarcomeres but also appears in other cellular components, indicating that extending our model could reveal additional mechanisms working across other biological hierarchies. Thus, our framework provides a basis for exploring the complex relationships between cellular physical structures and functions.

## **Acknowledgments**

Y.U. is supported by the Japan Society for the Promotion of Science (JSPS). This study was supported in part by JSPS KAKENHI grants (23H04929 and 24KJ1649).

## References

1. Zajac AL, Discher DE. Cell differentiation through tissue elasticity-coupled, myosin-driven remodeling. *Curr Opin Cell Biol.* 2008 Dec;20(6):609–15.
2. Discher DE, Janmey P, Wang YL. Tissue cells feel and respond to the stiffness of their substrate. *Science.* 2005 Nov 18;310(5751):1139–43.
3. Hove JR, Köster RW, Forouhar AS, Acevedo-Bolton G, Fraser SE, Gharib M. Intracardiac fluid forces are an essential epigenetic factor for embryonic cardiogenesis. *Nature.* 2003 Jan 9;421(6919):172–7.
4. Hahn C, Schwartz MA. Mechanotransduction in vascular physiology and atherogenesis. *Nature Reviews Molecular Cell Biology* 2009 10:1. 2009 Jan;10(1):53–62.
5. Henderson CA, Gomez CG, Novak SM, Mi-Mi L, Gregorio CC. Overview of the Muscle Cytoskeleton. *Compr Physiol.* 2017 Jul 1;7(3):891–944.
6. Purslow PP, Trotter JA. The morphology and mechanical properties endomysium in series-fibred muscles: variations with muscle length of. Vol. 15, *Journal of Muscle Research and Cell Motility.* 1994.
7. Reconditi M, Brunello E, Fusi L, Linari M, Martinez MF, Lombardi V, et al. Sarcomere-length dependence of myosin filament structure in skeletal muscle fibres of the frog. *J Physiol.* 2014 Mar 1;592(5):1119–37.
8. Ertbjerg P, Puolanne E. Muscle structure, sarcomere length and influences on meat quality: A review. *Meat Sci.* 2017 Oct 1;132:139–52.
9. Gollapudi SK, Lin DC. Experimental determination of sarcomere force-length relationship in type-I human skeletal muscle fibers. *J Biomech.* 2009 Sep 18;42(13):2011–6.
10. Herrera AM, McParland BE, Bienkowska A, Tait R, Paré PD, Seow CY. 'Sarcomeres' of smooth muscle: functional characteristics and ultrastructural evidence. *J Cell Sci.* 2005 Jun 1;118(11):2381–92.
11. Peterson LJ, Rajfur Z, Maddox AS, Freel CD, Chen Y, Edlund M, et al. Simultaneous stretching and contraction of stress fibers in vivo. *Mol Biol Cell.* 2004 Jul 7;15(7):3497–

508.

12. Verkhovsky AB, Svitkina TM, Borisy GG. Polarity sorting of actin filaments in cytochalasin-treated fibroblasts. *J Cell Sci.* 1997 Aug 1;110(15):1693–704.
13. Hotulainen P, Lappalainen P. Stress fibers are generated by two distinct actin assembly mechanisms in motile cells. *Journal of Cell Biology.* 2006 May 8;173(3):383–94.
14. Cramer LP, Siebert M, Mitchison TJ. Identification of Novel Graded Polarity Actin Filament Bundles in Locomoting Heart Fibroblasts: Implications for the Generation of Motile Force. *Journal of Cell Biology.* 1997 Mar 24;136(6):1287–305.
15. Deguchi S, Sato M. Biomechanical properties of actin stress fibers of non-motile cells. Vol. 46, *Biorheology.* 2009. p. 93–105.
16. Lazarides E, Burridge K. Alpha-actinin: immunofluorescent localization of a muscle structural protein in nonmuscle cells. *Cell.* 1975;6(3):289–98.
17. Coravos JS, Martin AC. Apical Sarcomere-like Actomyosin Contracts Nonmuscle *Drosophila* Epithelial Cells. *Dev Cell.* 2016 Nov 7;39(3):346–58.
18. Russell RJ, Grubbs AY, Mangroo SP, Nakasone SE, Dickinson RB, Lele TP. Sarcomere length fluctuations and flow in capillary endothelial cells. *Cytoskeleton.* 2011 Mar 1;68(3):150–6.
19. Goldspink G. Sarcomere length during post-natal growth of mammalian muscle fibres. *J Cell Sci.* 1968 Dec 1;3(4):539–48.
20. Vicente-Manzanares M, Ma X, Adelstein RS, Horwitz AR. Non-muscle myosin II takes centre stage in cell adhesion and migration. Vol. 10, *Nature Reviews Molecular Cell Biology.* 2009. p. 778–90.
21. Conti MA, Adelstein RS. Erratum: Nonmuscle myosin II moves in new directions (*Journal of Cell Science* vol. 121 (11-18)). Vol. 121, *Journal of Cell Science.* 2008. p. 404.
22. Schiffhauer ESS, Luo T, Mohan K, Srivastava V, Qian X, Griffis ERR, et al. Mechanoaccumulative Elements of the Mammalian Actin Cytoskeleton. *Current Biology.* 2016;26(11):1473–9.
23. Greenberg MJ, Arpağ G, Tüzel E, Ostap EM. A Perspective on the Role of Myosins as

- Mechanosensors. Vol. 110, *Biophysical Journal*. Biophysical Society; 2016. p. 2568–76.
24. Kolley F, Sidor C, Dehapiot B, Schnorrer F, Friedrich BM. Mechanisms of Sarcomere Assembly in Muscle Cells Inferred from Sequential Ordering of Myofibril Components. *PRX Life*. 2024 Jan 11;2(1).
  25. Friedrich BM, Fischer-Friedrich E, Gov NS, Safran SA. Sarcomeric pattern formation by actin cluster coalescence. *PLoS Comput Biol*. 2012;8(6).
  26. Katoh K, Kano Y, Masuda M, Onishi H, Fujiwara K. Isolation and contraction of the stress fiber. *Mol Biol Cell*. 1998 Oct 13;9(7):1919–38.
  27. Deguchi S, Ohashi T, Sato M. Tensile properties of single stress fibers isolated from cultured vascular smooth muscle cells. *J Biomech*. 2006 Jan 1;39(14):2603–10.
  28. Crooks GE. Entropy production fluctuation theorem and the nonequilibrium work relation for free energy differences. 1999;
  29. Deguchi S, Ohashi T, Sato M. Tensile properties of single stress fibers isolated from cultured vascular smooth muscle cells. *J Biomech*. 2006 Jan 1;39(14):2603–10.
  30. Lovett DB, Shekhar N, Nickerson JA, Roux KJ, Lele TP. Modulation of nuclear shape by substrate rigidity. *Cell Mol Bioeng*. 2013 Jun 5;6(2):230–8.
  31. Newman J, oczka N, Schick KL. Dynamic light scattering measurements of the diffusion of probes in filamentous actin solutions. *Biopolymers*. 1989 Feb 1;28(2):655–66.
  32. Montague C, Rhee KW, Carlson FD. Measurement of the translational diffusion constant of G-actin by photon correlation spectroscopy. *J Muscle Res Cell Motil*. 1983 Feb;4(1):95–101.
  33. Kanzaki N, Uyeda TQP, Onuma K. Intermolecular interaction of actin revealed by a dynamic light scattering technique. *Journal of Physical Chemistry B*. 2006 Feb 16;110(6):2881–7.
  34. Kodama T, Woledge RC. Enthalpy changes for intermediate steps of the ATP hydrolysis catalyzed by myosin subfragment-1. *Journal of Biological Chemistry*. 1979;254(14):6382–6.
  35. Gajewski E, Steckler DK, Goldberg RN. Thermodynamics of the hydrolysis of adenosine 5'-triphosphate to adenosine 5'-diphosphate. *Journal of Biological Chemistry*.

1986;261(27):12733–7.

36. Balnave CD, Davey DF, Allen DG. Distribution of sarcomere length and intracellular calcium in mouse skeletal muscle following stretch-induced injury. *Journal of Physiology*. 1997 Aug 1;502(3):649–59.
37. Manabe Y, Ogino S, Ito M, Furuichi Y, Takagi M, Yamada M, et al. Evaluation of an in vitro muscle contraction model in mouse primary cultured myotubes. *Anal Biochem*. 2016 Mar 15;497:36–8.
38. Burbaum L, Schneider J, Scholze S, Böttcher RT, Baumeister W, Schwille P, et al. Molecular-scale visualization of sarcomere contraction within native cardiomyocytes. *Nature Communications* 2021 12:1. 2021 Jul 2;12(1):1–12.
39. Ishiwata S, Okamura N. Diffraction rings obtained from a suspension of skeletal myofibrils by laser light illumination. Study of internal structure of sarcomeres. *Biophys J*. 1989 Dec 1;56(6):1113–20.
40. Sanger JW, Sanger JM, Jockusch BM. Differences in the Stress Fibers Fibroblasts and Epithelial Cells between. Vol. 96, *THE JOURNAL OF CELL BIOLOGY*. 1983.
41. Matsui TS, Kaunas R, Kanzaki M, Sato M, Deguchi S. Non-muscle myosin II induces disassembly of actin stress fibres independently of myosin light chain dephosphorylation. *Interface Focus*. 2011;1(5):754–66.
42. Costa KD, Hucker WJ, C-P Yin F. Buckling of Actin Stress Fibers: A New Wrinkle in the Cytoskeletal Tapestry. 2002;
43. Katoh K, Kano Y, Masuda M, Onishi H, Fujiwara K. Isolation and contraction of the stress fiber. *Mol Biol Cell*. 1998 Oct 13;9(7):1919–38.
44. Kentish JC, Ter Keurs HEDJ, Ricciardi L, Bucx JJ, Noble MI. Comparison between the sarcomere length-force relations of intact and skinned trabeculae from rat right ventricle. Influence of calcium concentrations on these relations. *Circ Res*. 1986;58(6):755–68.
45. Azzabou N, Hogrel JY, Carlier PG. NMR based biomarkers to study age-related changes in the human quadriceps. *Exp Gerontol*. 2015 Oct 1;70:54–60.
46. Shannon CE, Weaver W. *THE MATHEMATICAL THEORY OF COMMUNICATION*. 1949;

47. Foley KS, Young PW. An analysis of splicing, actin-binding properties, heterodimerization and molecular interactions of the non-muscle  $\alpha$ -actinins. *Biochemical Journal*. 2013 Jun 15;452(3):477–88.
48. Meyer RK, Aebi U. Bundling of actin filaments by alpha-actinin depends on its molecular length. *Journal of Cell Biology*. 1990 Jun 1;110(6):2013–24.
49. Wachsstock DH, Schwartz WH, Pollard TD. Affinity of alpha-actinin for actin determines the structure and mechanical properties of actin filament gels. *Biophys J*. 1993;65(1):205–14.
50. Van Dijk J, Furch M, Lafont C, Manstein DJ, Chaussepied P. Functional characterization of the secondary actin binding site of myosin II. *Biochemistry*. 1999 Nov 16;38(46):15078–85.



# Figures

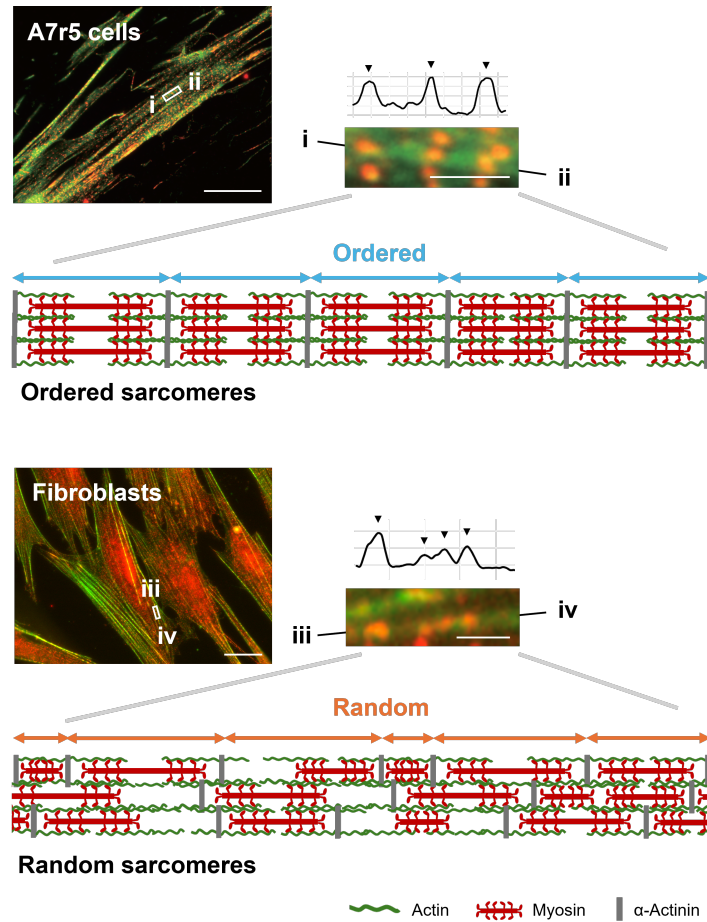


Fig.1 Schematic of sarcomere structure. The upper diagram (blue) shows the cytoskeleton with ordered sarcomeres of specific lengths, characterized by stable tension maintenance. The lower diagram (orange) shows the cytoskeleton with random sarcomeres of varying lengths, characterized by flexible adaptability to environmental changes.

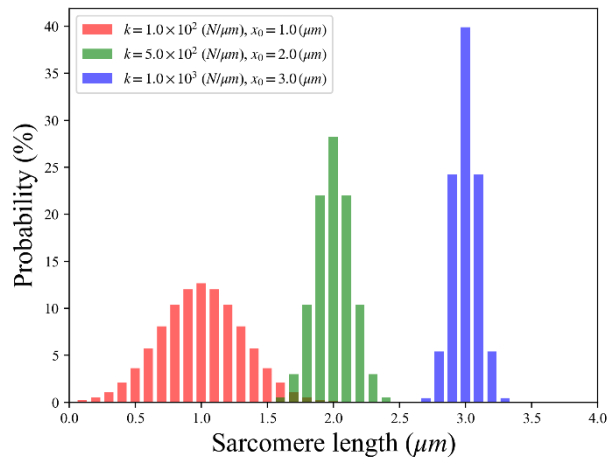


Fig.2 Length distribution of sarcomeres at  $k = 10^2$  [N/μm] (red),  $10^3$  [N/μm] (green), and  $10^4$  [N/μm] (blue). With a smaller  $k$ , the distribution of sarcomere lengths exhibits greater variability, indicating increased structural diversity.

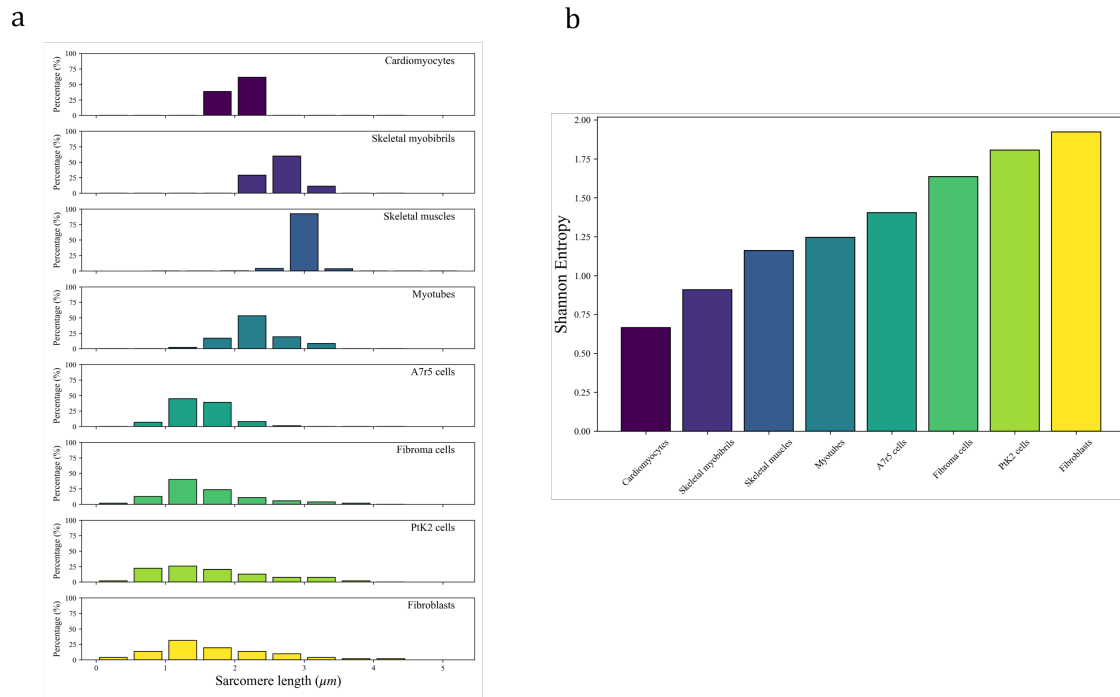


Fig.3 Quantification of sarcomere length variability. (a) The actual sarcomere length was quantified using previously published experimental images from multiple sources. (b) Shannon entropy was calculated for each distribution.

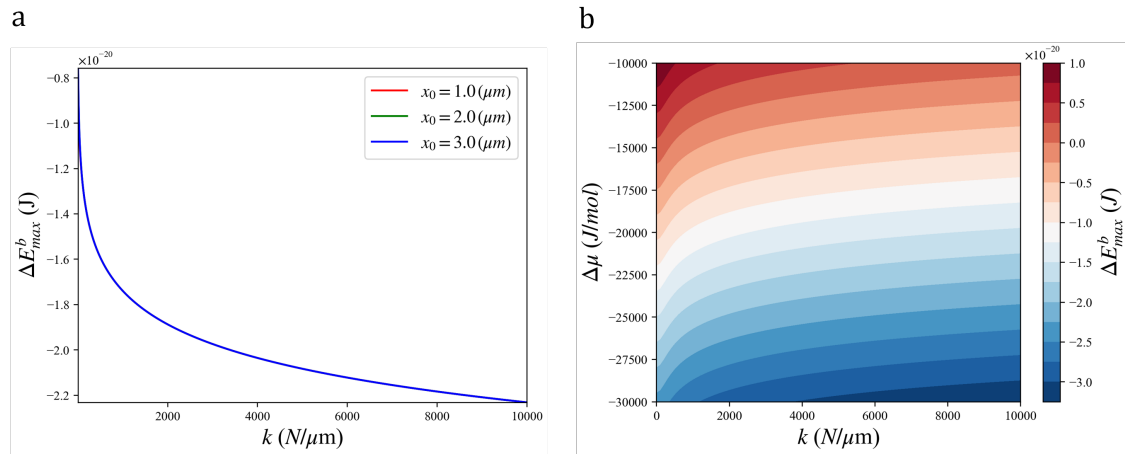


Fig.4 Maximum binding energy condition between sarcomeres. (a) Relation between restoring contribution and maximum binding energy. A higher restoring contribution corresponds to a lower maximum binding energy, indicating higher binding between sarcomeres. (b) Dependence of maximum binding energy on restoring contribution and chemical potential. A lower chemical potential results in a lower maximum binding energy.

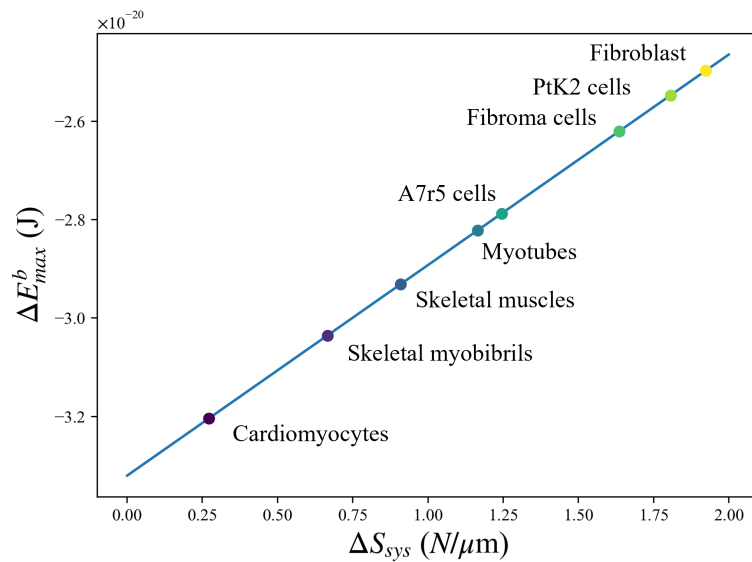


Fig.5 Estimation of binding energy for different sarcomere structures. The binding energy for different types of sarcomere structures was estimated using Eq. (8) and the distributions shown in Fig. 3 at a fixed chemical potential of -20 kJ/mol.